MOLECULAR IMAGING AND BIOLOGY

Mol Imaging Biol (2014)
DOI: 10.1007/s11307-014-0742-3
© World Molecular Imaging Society, 2014

World Molecular Imaging Society

RESEARCH ARTICLE

Near-Infrared Fluorescence Imaging of Non-Hodgkin's Lymphoma CD20 Expression Using Cy7-Conjugated Obinutuzumab

Xinfeng Lin,[1] Hua Zhu,[1] Zheng Luo,[1] Ye Hong,[2] Hong Zhang,[3] Xijuan Liu,[3] Huirong Ding,[3] Huifang Tian,[3] Zhi Yang[1]

[1]*Key Laboratory of Carcinogenesis and Translational Research (Ministry of Education), Department of Nuclear Medicine, Peking University Cancer Hospital & Institute, 52 Fucheng Road, Haidian District, 100142, Beijing, China*
[2]*China Institute of Atomic Energy, 102413, Beijing, China*
[3]*Key Laboratory of Carcinogenesis and Translational Research (Ministry of Education), Central Laboratory, Peking University Cancer Hospital & Institute, 100142, Beijing, China*

Abstract

Purpose: Obinutuzumab is the first fully humanized and glycoengineered monoclonal antibody (mAb) directly targeting CD20 antigen, which is expressed on B cell lymphocytes and the majority of non-Hodgkin's lymphoma (NHL). This study aims to design a diagnostic molecular probe, Cy7-Obinutuzumab (Cy7-Obi), in which Cy7 is a near-infrared fluorescent dye. This probe is used to noninvasively image CD20 antigen expressed in NHL cells.

Procedures: Cy7-Obi probe was synthesized through nucleophilic substitution reaction between NHS-Cy7 and obinutuzumab. After purification, the conjugate was fully characterized by a series of methods. The immunoreactivity and molecular specificity of the probe were confirmed using flow cytometry and *in vitro* microscopy on Raji (CD20-positive) cells. For *in vivo* imaging, Cy7-Obi probe (1 nmol) was injected intravenously in severe combined immunodeficiency (SCID) mice bearing Raji tumors which overexpress CD20 (n=3) and was imaged with near-infrared fluorescence (NIRF) at 6, 9, 12, 24, 60, and 96 h post-probe injection. For pre-block, obinutuzumab (3.25 mg) was injected intravenously in tumor-bearing mice 6 h before the administration of Cy7-Obi probe.

Results: The synthesized Cy7-Obi probe in this paper mimics obinutuzumab in both structure and function. Flow cytometry analysis of the probe and obinutuzumab on Raji cells showed minor difference in binding affinity/specificity with CD20. The probe showed significant fluorescence signal when it was examined on Raji cells using *in vitro* microscopy. The fluorescence signal can be blocked by pretreatment with obinutuzumab. The probe Cy7-Obi also showed high tumor uptake when it was examined by *in vivo* optical imaging on Raji tumor-bearing mice. The tumor uptake can be blocked by pretreatment with obinutuzumab (n=3, $p<0.05$). The *in vivo* imaging results were also confirmed by *ex vivo* imaging of dissected organs. Finally, the probe Cy7-Obi has shown excellent tumor targeting and specificity through immunofluorescence analysis.

Xinfeng Lin and Hua Zhu contributed equally to this study.

Electronic supplementary material The online version of this article (doi:10.1007/s11307-014-0742-3) contains supplementary material, which is available to authorized users.

Correspondence to: Zhi Yang; *e-mail:* pekyz@163.com

Published online: 16 May 2014

Conclusions: We have shown that humanized Cy7-Obi probe can be used for NIRF imaging successfully. The probe may be an effective and noninvasive diagnostic molecular probe capable of tracking CD20 overexpression in NHL.

Key words: Near-infrared fluorescence imaging, Cyanine dye indotricarbocyanine, CD20, Obinutuzumab, Non-Hodgkin's lymphoma

Introduction

Non-Hodgkin's lymphoma (NHL) is the seventh most common cancer in the USA, and its incidence has increased by 15 % over the past two decades. According to the latest cancer statistics by the American Cancer Society, about 37,600 new cases and approximately 10,590 deaths of NHL are projected to occur in the USA in 2013 [1]. In China, the cancer statistics provided by Chinese Anti-Cancer Association reveal that about 84,000 cases and approximately 47,000 deaths of lymphoma occur annually, and the incidence will be increasing by 5 % annually in the future. The NHL patients account for 85–90 % in all lymphoma patients, and the proportion is higher than that in countries of Europe and the USA [2]. NHL is a heterogeneous group of diseases of B cell or T cell origin, of which 85 % are of B cell origin, among which a majority has high level expression of CD20 antigens [3].

CD20 antigens are regarded as unique markers of B cells and play a role in B cell activation and proliferation [4]. CD20 is a member of the multispanning 4A (MS4A) family of tetraspanins consisting of 297 amino acids and unglycosylated phosphoproteins with molecular weight of 33–36 kD [5, 6]. There is no clear evidence implying that CD20 antigens tend to shed from the cell surface or be internalized after antibody binding, and no free antigens can be found circulating in blood plasma [7–9]. CD20 is B cell-restricted differentiation antigen and expressed within key B cell development. Besides normal B lymphocytes, CD20 antigens are also expressed on B cell lymphoma tissues, such as B cell NHL and chronic lymphocytic leukaemia (CLL), while CD20 expression level varies from kinds of leukaemia [10].

Rituximab and obinutuzumab are humanized monoclonal antibodies (mAbs) specifically directed against the CD20 antigen-expressing B cell lymphomas. The differences between the two antibodies exist in different aspects, such as the degree of humanization, the effect of complement-dependent cytotoxicity and antibody-dependent cell-mediated cytotoxicity, and so on [11]. As a third-generation anti-CD20 mAb, obinutuzumab is the first fully humanized and glycoengineered type II protein [12]. The degree of humanization of obinutuzumab is higher than that of rituximab, which reduces immunogenicity [13]. However, rituximab has been approved by the Food and Drug Administration (FDA) for therapy alone or in combination, while obinutuzumab is currently undergoing clinical trial. As a result, studies on the basis of rituximab for tumor diagnosis and therapies prevail.

A series of imaging agents based on rituximab (Rit) and related mAbs have been developed to monitor NHL therapy or for diagnosis, such as positron emission tomography (PET) imaging and single photon emission computed tomography (SPECT) imaging. The SPECT imaging agent, ^{99m}Tc-rituximab [14], specifically accumulates in the tumor region post-injection, suitable to serve as an effective imaging diagnostic method to evaluate CD20 expression level in NHL patients [15]. PET imaging agents, such as those of Rit labeled with ^{64}Cu and ^{124}I, have promising imaging applications for B cell lymphomas [16–18]. Both imaging techniques are highly sensitive, and their images show deep tissue penetration; however, they require radiolabeled compounds which may be expensive to synthesize (PET) or provide radiation dose due to the emission of gamma rays. As a result, optical imaging techniques such as near-infrared fluorescence (NIRF) imaging have recently been developed for tumor diagnosis.

Optical imaging, especially NIRF imaging, has proved to be a powerful tool for studying molecular basis of disease states [19–24]. An inspiring news came from Netherlands Cancer Institute was that NIRF imaging had been successfully used to facilitate and optimize dissection of sentinel lymph nodes during robot-assisted laparoscopic prostatectomy procedures [25]. In this study, we report the results of a new near-infrared molecular probe Cy7-Obi based on the third-generation anti-CD20 mAb obinutuzumab. The probe was fully characterized by a variety of chemical and biological analysis, including animal imaging studies (*in vivo* and *ex vivo*). It showed promise as a new probe for NHL diagnosis.

Materials and Methods

Materials

The anti-CD20 antibody obinutuzumab was purchased from Roche (Basle Switzerland). Fluorescein isothiocyanate (FITC)-conjugated goat anti-human IgG was obtained from GE Healthcare (Piscataway, NJ, USA). Murine monoclonal antibody IgG was purchased from Gene Tech (Shanghai) Company Limited (Shanghai, China). *N*,*N*-dimethylformamide (DMF) was from J&K Scientific Ltd (Shanghai, China). Monofunctional hydroxysuccinimide of indocyanine 7 (Cy7-NHS) was obtained from Lumiprobe Corporation (Hallandale Beach, FL, USA). All chemicals and solvents used were purchased from Sinopharm Chemical Reagent Co., Ltd (Shanghai, China) unless otherwise

stated. Mass spectrometry (Ultraflex III, Bruker Daltonics, Bremen, Germany) and laser scanning confocal microscope (LSCM, Leica TCS SP5 X, Solms, Germany) were performed at Peking University Cancer Hospital and operated in a linear mode with sinapinic acid matrix. Small animal imaging system (Xenogen IVIS™ 200, Xenogen, Alameda, CA, USA) was performed at Peking University Cancer Hospital. UV–vis spectrophotometer (NanoDrop 2000/2000c, Thermo Fisher Scientific, USA) was used to determine some solution concentrations. Disposable PD-10 Desalting Columns (PD-10 columns) were purchased from GE Healthcare (Piscataway, NJ, USA).

Synthesis and Purification of Cy7-Obi Conjugates

The protocol for the conjugation of Cy7-NHS and obinutuzumab was used with some modifications [26]. Briefly, obinutuzumab (0.6 mg) in 60 µl of 1 M sodium bicarbonate ($NaHCO_3$) buffer (pH=8.2) was mixed with Cy7-NHS (0.03 µmol) in 20 µl of DMF and 120 µl of 1 M $NaHCO_3$ buffer (1 mol/l, pH=8.2). The reaction vessel was wrapped under aluminum foil, and the mixture was allowed to warm up to RT (25 °C) and to react for 4 h. After the reaction was complete, the reaction mixture was loaded on a PD-10 column (Disposable PD-10 Desalting Columns Improved) and prerinsed five times with phosphate buffer solution (PBS) buffer (0.01 M, pH=7.4). The synthesized product was collected after elution using 0.01 M PBS buffer (pH=7.4).

Characterization of Cy7-Obi

Absorption Spectrum of Cy7-Obi The UV–vis absorbance peaks of Cy7-NHS, obinutuzumab, and Cy7-Obi were determined at the wavelengths of 280 and 750 nm, respectively, by scanning the wavelength which ranged from 200 to 850 nm.

Number of Cy7-NHS Conjugated to Obinutuzumab (F/P Ratio)

The number of fluorochrome molecules per molecule of protein is known as the *F*/*P* ratio, which is an important contributor in the biological properties of the conjugates [27–29]. The ratio was determined by measuring the absorbance of Cy7-NHS at or near its characteristic excitation maximum (~750 nm).

Mass Spectrometry Analysis of Cy7-Obi

Both obinutuzumab and Cy7-Obi were prepared at 20 µl (2 mg/ml). The samples were then diluted to approximately 1.0 mg/ml by the addition of 0.1 % trifluoroacetic acid in water. Sinapinic acid at 10 mg/ml in 50/50 acetonitrile/H_2O with 0.1 % TFA was used as the matrix of matrix-assisted laser desorption/ionization (MALDI). One microliter of mixture (1:1) between the above-prepared sample and matrix was used for mass analysis. The spectrum was acquired in a positive linear mode and analyzed using the FlexAnalysis v3.0 software.

Cell Culture

Burkitt's lymphoma Raji cell line and lung carcinoma A549 cell line were obtained from American Type Culture Collection (Manassas, VA, USA) and were cultured at 37 °C in an incubator in a humidified atmosphere containing 5 % CO_2. The medium for the cell was Roswell Park Memorial Institute (RPMI) medium 1640, supplemented with 10 % fetal bovine serum, 2 mmol/l glutamine, and 100 U/ml penicillin. All medium and additives were purchased from Life Technologies Incorporation (Grand Island, NY, USA).

In Vitro Cell Study and In Vitro Flow Cytometry

A total of 5×10^6 Raji cells were harvested and suspended in cold PBS (0.01 M, pH 7.4) with 1 % fetal calf serum. The cells were incubated with obinutuzumab or Cy7-Obi (5 µg/ml), the primary antibody to CD20, for 30 min at 37 °C in the dark, washed three times with PBS, and then the cell suspension was centrifuged at 1,000 rpm for 5 min. The cell pellets were resuspended in PBS. After incubation with the appropriate FITC-conjugated goat anti-human IgG for 1 h at 37 °C in the dark, the cells were washed twice and resuspended in cold PBS. The cell samples were finally analyzed by BD Accuri C6 Flow Cytometer (Becton-Dickinson, San Jose, CA), which is equipped with 488- and 633-nm lasers and FlowJo analysis software (Tree Star, Inc., Ashland, OR).

In Vitro Microscopy

Raji cells were cultured to the logarithmic phase and then were incubated with appropriate Cy7-Obi (100 µg) in cell culture medium at 37 °C. For the blocking study, 2 mg cold obinutuzumab was added 30 min prior to the addition of Cy7-Obi. After incubation for 30 min, the cells were washed three times with cold PBS (0.01 M, pH 7.4). Fluorescence microscopy experiments were performed by using a Leica DMI3000B fluorescence microscope (Leica Microsystem Wetzlar, Inc., Wetzlar, Germany). A custom Cy7 filter set was used (excitation, 750/30 nm; emission, 780/30 nm).

Animal Study and Animal Models

Male SCID mice (4–6 weeks of age) were purchased from Vital River Laboratory Animal Technology Co., Ltd (Beijing, China) and maintained under pathogen-free conditions. The animals were housed in five per cage and provided with sterilized pellet chow and sterilized water at Specific Pathogen Free (SPF) Animal Lab at Peking University Cancer Hospital. The facility is accredited by the Beijing Administration Office of Laboratory Animal, and all experiments were implemented in accordance with the guidelines of the Institutional Animal Care and Use Committee of Peking University. Before implantation, Raji cells were centrifuged at 1,000 rpm for 5 min and then resuspended in sterile physiological saline. Raji cells (2×10^6–5×10^6 per animal) were implanted subcutaneously into the right axilla of the mice. The optical imaging was performed after the tumor reached 1–2 cm in diameter.

In Vivo and Ex Vivo NIRF Imaging

Mice were anesthetized with 2 % isoflurane gas (Iso-Thesia, Rockville, NY) in oxygen. During imaging, mice were maintained in an anesthetized state with 0.5–1.5 % isoflurane. The hair of the right axilla of all mice was shaved to avoid laser scattering.

A Xenogen IVIS™ 200 small animal imaging system with a Cy7 filter set (excitation, 750/30 nm; emission, 780/30 nm) was used in this study. All the fluorescence images were acquired with 5 s exposure and were normalized by dividing the fluorescent images by reference illumination images. Regions of interest (ROIs) were drawn on tumor regions, and the average radiant efficiency (presented as mean±SD in the unit of $[p/s/cm^2/sr]/[\mu W/cm^2]$) within the ROI was used for subsequent quantitative analysis. Mice (n=3) from two groups were injected intravenously with 1 nmol Cy7-Obi. For the evaluation of CD20 receptor specificity of Cy7-Obi *in vivo*, blocking studies were carried out. A group of three mice was each injected with 3.25 mg of obinutuzumab 6 h before Cy7-Obi administration. All mice were imaged at various times (6, 9, 12, 24, 60, and 96 h) post-injection (p.i.). For *ex vivo* studies, the tumors and major organs were dissected and imaged again at 96 h p.i..

Serum Stability

The tracer was incubated at 4 °C in complete fetal bovine serum. After a certain time, the solution containing Cy7-Obi would be purified by PD-10 columns, and any free Cy7 molecules generated by fracturing of the bond between Cy7 molecule and mAb would be washed out. Thus, the fluorescence intensity originated from Cy7-Obi could be measured by using a Xenogen IVIS™ 200 small animal imaging system with a Cy7 filter set. Excitation wavelength was set at 750 nm, and emission scan range was 770–790 nm. The fluorescence intensity at 780 nm was plotted against time, to examine the image agent stability in serum.

Histology

In order to study image agent's specificity to CD20 antigens in tumor tissue, an extra Raji tumor-bearing mouse, used as a control, was intravenously injected with a murine monoclonal antibody IgG (5 mg). At 96 h p.i., mice were executed and tumors accumulated with either kind of primary antibody (IgG or Cy7-Obi), were made frozen, and were sliced at 5–10 μm thickness. All slices were fixed with acetone for 10 min and dried in air for 30 min. The slides were placed in a rack, which were placed in a tank filled with PBS and washed for 5–10 min. After blocking with 20 % fetal bovine serum (FBS)–PBS for 30 min, the slices were incubated with FITC-conjugated goat anti-human IgG as second antibody for 1 h at 37 °C in the dark and were washed with PBS three times and were incubated in a solution of 4′,6-diamidino-2-phenylindole (DAPI) in 95 % ethanol for 30 min to fix and stain cell nuclei.

Statistics Analysis

Statistical analysis was performed with SPSS software (version 17.0; SPSS Institute Inc.). One-way analysis of variance (ANOVA) for statistical evaluation was performed. All data are given as means±SD, and means were compared using Student's t test. A P value of <0.05 was considered to be statistically significant.

Results

Synthesis and Characterization of Cy7-Obi Conjugate

Cy7-Obi conjugate was synthesized by coupling of Cy7-NHS with N-terminal amines in obinutuzumab following the method reported [26, 30]. After purification, the conjugate was characterized by a series of methods described below.

Absorption Spectrum of Cy7-Obi

The newly synthesized conjugate, Cy7-Obi, had two absorbance peaks centered around 280 and 750 nm as shown in Electronic Supplementary Material (ESM) Fig. 1c. The absorption spectra of Cy7-NHS showed no peak around 280 nm, while a peak was observed around 750 nm (ESM Fig. 1a). Obinutuzumab showed a peak around 280 nm, while no peak was observed around 750 nm (ESM Fig. 1b). Although the absorption has almost identical peak positions, the peaks have quite different absorption coefficients [31].

Number of Cy7 Unit in the Conjugate Cy7-Obi (F/P Ratio)

The F/P ratio was calculated through the comparison of absorbance coefficients at the two peaks of the conjugate. The absorbance of Cy7-Obi solution was measured at the wavelengths of 280 and 750 nm, respectively. The molar extinction coefficients of Cy7-NHS and obinutuzumab at 280 and 750 nm are 1.7×10^5 l mol^{-1} cm^{-1} (280 nm) and 2×10^5 l mol^{-1} cm^{-1} (750 nm) in a buffer of pH 8.2. According to the Lambert-Beer law $A=\varepsilon\cdot b\cdot c$ (b=0.1 cm, ε = molar extinction coefficient, unit: l mol^{-1} cm^{-1}, c = molality, unit: mol/l), the following formulas can be obtained:

$$n[\mathrm{Cy7}] = (A_{750})/200,000$$

$$n[\mathrm{obinutuzumab}] = [A_{280} - (0.0146 \times A_{750})]/170,000$$

$$F/P = n[\mathrm{Cy7\ \ dye}]/n[\mathrm{obinutuzumab}]$$
$$= (0.85 \times A_{750})/[A_{280} - (0.0146 \times A_{750})].$$

Here, the 1.46 % of absorbance at 750 nm represents the contribution of Cy7 moiety at 280 nm in the conjugate. The

F/*P* ratio was determined to be 1.010, meaning that about one molecule of Cy7-NHS was conjugated to one molecule of obinutuzumab.

Estimation of Cy7-NHS Conjugated to Obinutuzumab by Mass Spectrometry

The number of Cy7 moiety within the conjugate Cy7-Obi was measured by the measurement of the molecule weight of the conjugate using mass spectrometry. The MALDI-time of flight (TOF) mass spectrometry showed that the molecular weights of obinutuzumab and Cy7-Obi were at ~148,909.688 Da (Fig. 1a) and 149,597.433 Da (Fig. 1b), respectively. The mass difference between the two peaks at ~150 kD region was *m*/*z* 687.745, corresponding to one unit of Cy7 moiety per obinutuzumab (absolute mass of Cy7-NHS *m*/*z* is 682.29). This confirmed that the number of Cy7-NHS reacting with obinutuzumab was about 1, consistent with the calculation described above from UV–vis measurement (Fig. 1).

In Vitro Cell Study and In Vitro Flow Cytometry

In vitro flow cytometry analysis of Raji cells showed that the conjugate maintained the binding affinity of obinutuzumab. Raji cells were previously confirmed to have CD20 expression [32, 33]. After the conjugate and obinutuzumab were combined with the cells, FITC-conjugated goat anti-human IgG showed that they had similar binding affinity to CD20 using flow cytometry (Fig. 2), indicating that the conjugation did not alter the affinity of obinutuzumab.

We have also examined the specificity of the conjugate to CD20 on Raji cells and A549 cells without CD20 expression. The two kinds of cell lines were first incubated with the primary antibody conjugate Cy7-Obi and then with secondary FITC-conjugated goat anti-human IgG. The fluorescent intensity of Raji cells obtained by flow cytometry was much higher than that of A549 cells (data not shown), meaning that Cy7-Obi could specifically recognize CD20 (Fig. 2).

In Vitro Microscopy

The specificity and binding affinity of Cy7-Obi to CD20 antigen were embodied directly by the fluorescence microscopy images. Significant fluorescence signal was observed for cells incubated with Cy7-Obi. In contrast, fluorescence signal nearly disappeared when the cells were pretreated with a blocking dose of obinutuzumab (Fig. 3).

In Vivo and Ex Vivo NIRF Imaging

A series of representative *in vivo* NIRF images and quantitative data obtained from ROI analysis show that Cy7-Obi in tumor was clearly observable 6 h p.i. and had a maximal value at 24 h p.i. (Fig. 4a). After mice bearing

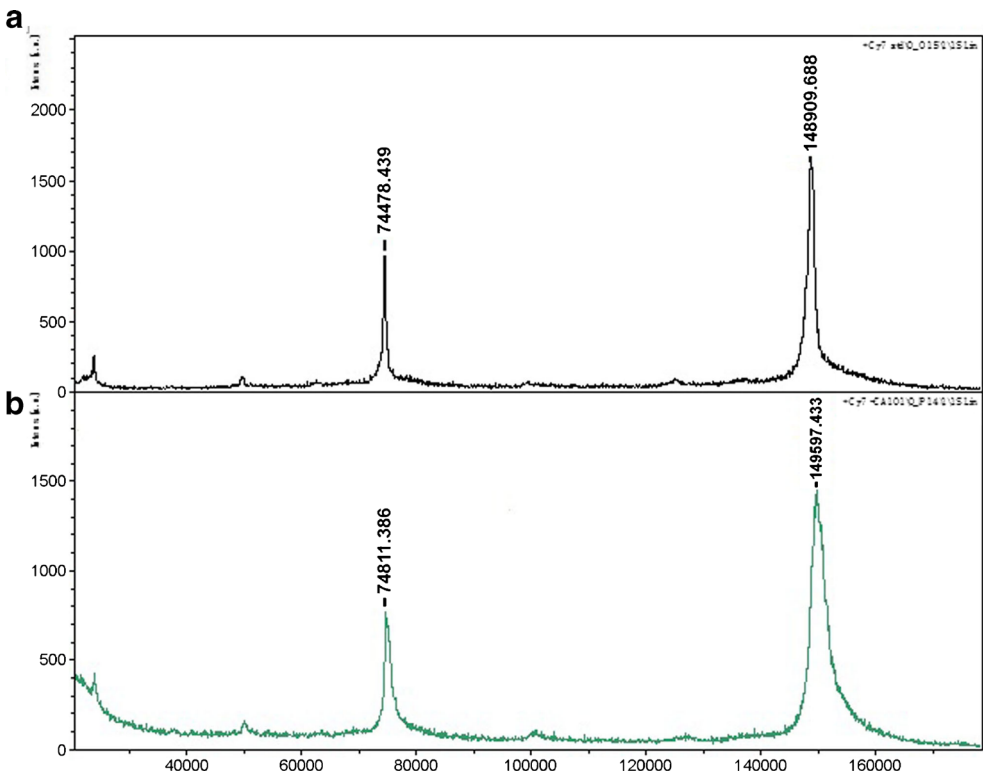

Fig. 1 Estimation of number of Cy7-NHS molecules conjugated to obinutuzumab by mass spectrometry. MALDI-TOF mass spectra of unmodified obinutuzumab (**a**) and Cy7-Obi conjugate (**b**).

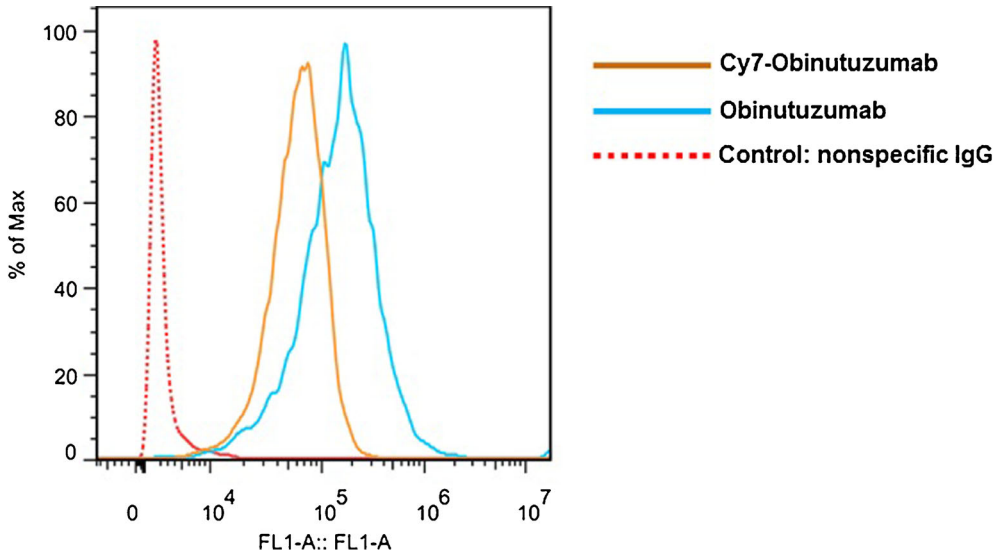

Fig. 2 Flow cytometry was used to evaluate the binding affinity of Cy7-Obi to CD20. Raji cells overexpressing CD20 showed strong fluorescence signal of similar intensity after incubating with obinutuzumab (*light blue-colored straight line*) and Cy7-Obi (*mustard-colored straight line*), as compared with control group cells (*red dotted line*).

subcutaneous Raji tumors were intravenously injected with Cy7-Obi with or without pre-doses of cold obinutuzumab at the dose of 1 nmol/mouse, near-infrared fluorescent images were recorded at various times (6, 9, 12, 24, 60, and 96 h) post-injection. The time–activity curve of the tumor at the baseline follows that of the typical fluorescence ligand, with a relatively fast uptake followed by washout (Fig. 4b). The maximal uptake occurred at about 24 h p.i. [$(4.23\pm0.53)\times10^7$, $(4.94\pm0.05)\times10^7$, $(5.41\pm0.75)\times10^7$, $(5.81\pm0.79)\times10^7$, $(5.16\pm0.55)\times10^7$, and $(4.51\pm1.24)\times10^7$ [p/s/cm^2/sr]/[μW/cm^2] at 6, 9, 12, 24, 60, and 96 h p.i.)]. When the mice were blocked by pretreatment with 3.25 mg obinutuzumab before Cy7-Obi administration, the time–activity curve of the tumor follows a similar pattern as that at the baseline (Fig. 4b) but at a much reduced level of radioactivity [$p<0.05$; $(2.54\pm0.61)\times10^7$, $(2.66\pm0.70)\times10^7$, $(3.38\pm1.15)\times10^7$, $(3.88\pm1.57)\times10^7$, $(3.34\pm0.03)\times10^7$, and $(3.15\pm0.87)\times10^7$ [p/s/cm^2/sr]/[μW/cm^2] at 6, 9, 12, 24, 60, and 96 h p.i.].

The results from *in vivo* NIRF images were also confirmed by *ex vivo* studies (Fig. 4c, d). After the mice bearing Raji tumor were euthanized 96 h p.i., major organs were dissected, arranged within a dish, and measured using NIRF imaging. The fluorescence intensity of different organs 96 h p.i. with and without pre-blocking by obinutuzumab showed that the biodistribution of Cy7-Obi is highly uneven especially in tumor ($p<0.05$, Fig. 4d), with the highest at Raji tumor, followed by the liver. This study also shows that the uptake at tumor can be blocked by pretreatment with obinutuzumab (Fig. 4).

Histology

The immunofluorescence staining of tumor tissue slices shows that the conjugate Cy7-Obi specifically accumulated in Raji tumor tissue. The indirect immunofluorescence analysis is always used to detect the primary antibody existing in various kinds of tissues and has the advantages of high sensitivity, specificity, and accurate positioning [34]. After *in vivo* NIRF image, the Raji tumor tissue with Cy7-Obi was dissected and sliced. FITC-conjugated goat anti-human IgG recognized the location of Cy7-Obi (Fig. 5b, c, and f), while it did not show murine monoclonal antibody IgG which covered the CD20 antigen (Fig. 5e). This is consistent with the observation of the *in vitro* microscopy study described above (Fig. 5).

Serum Stability

The fluorescence signal of Cy7-Obi in serum was stable up to 4 days, with intensity decrease less than 5 % (ESM Fig. 2).

Discussion

Recent studies of rituximab-based medicine imaging agents have generated many useful agents [14–16, 19, 35, 36]. For example, the conjugate, Cy5.5-rituximab [19], selectively accumulated in the tumor tissue and major excretion organs of mice bearing lymphoid tumor xenograft. Recently, we have synthesized and evaluated the molecular probe Cy7-rituximab [35]. *In vivo* fluorescence imaging showed specific concentration of the tracer in the spleen organ which is known to express high levels of CD20 antigens.

We selected obinutuzumab, the third-generation of anti-CD20 mAb, to be the target agent to bind with CD20. Compared to rituximab, obinutuzumab has higher degree of humanization, which can decrease the immunogenicity when applied to human [13]. We also selected the NIRF moiety

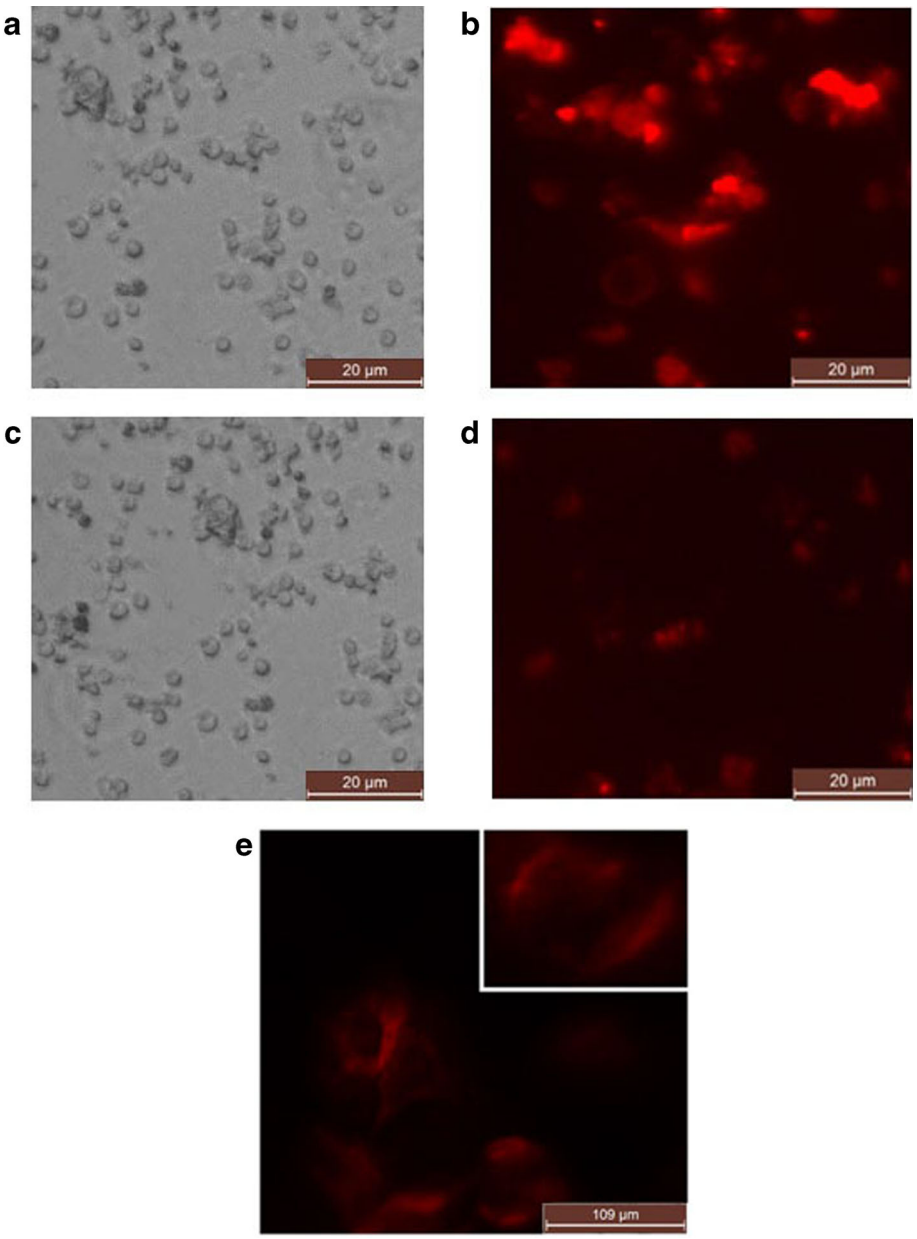

Fig. 3 Fluorescence microscopy images of Raji cells after incubating with 100 μg Cy7-Obi without **a** brightfield images and **b** fluorescence images with 2 mg obinutuzumab as blocking agent (**c** brightfield images, **d** fluorescence images). **e** Magnified view of some and one of (*right top corner*) representative cells.

Cy7-NHS, to be part of imaging agent. NIRF means electromagnetic in the wavelength range of 650 to 900 nm. In this wavelength range, the absorbance and autofluorescence spectra for water and biomolecules (such as serum albumin) are minimal, thus allowing for deep tissue penetration with minimal intra-tissue light scattering [37]. Thus, the conjugate, Cy7-Obi, has specific binding analogous to obinutuzumab, and as a potential NIRF imaging agent, it obtains the strong tissue penetration and noninvasion properties because of the conjugated Cy7-NHS dye.

We have optimized the conjugation of Cy7-NHS and obinutuzumab, to achieve optimal F/P ratio. Since fluorescence resonance energy transfer only occurs when two fluorophores are within 10 nm (about the size of an antibody), one or less than one Cy7 dye per antibody (that is $F/P \leq 1$) is needed to avoid self-quenching and to improve fluorescence signal [38]. Moreover, our experiments showed that large loss of affinity to CD20 occurred if obinutuzumab was labeled with lots of Cy7 dye molecules, and the fluorescence signal could not reach its potential if F/P ratio was much less than 1. We have achieved the F/P ratio 1.010, close to optimal value desirable for such imaging agent.

The conjugate Cy7-Obi was fully characterized by absorption spectrum, mass spectrometry, and sodium dodecyl sulfate polyacrylamide gel electrophoresis (SDS-PAGE)

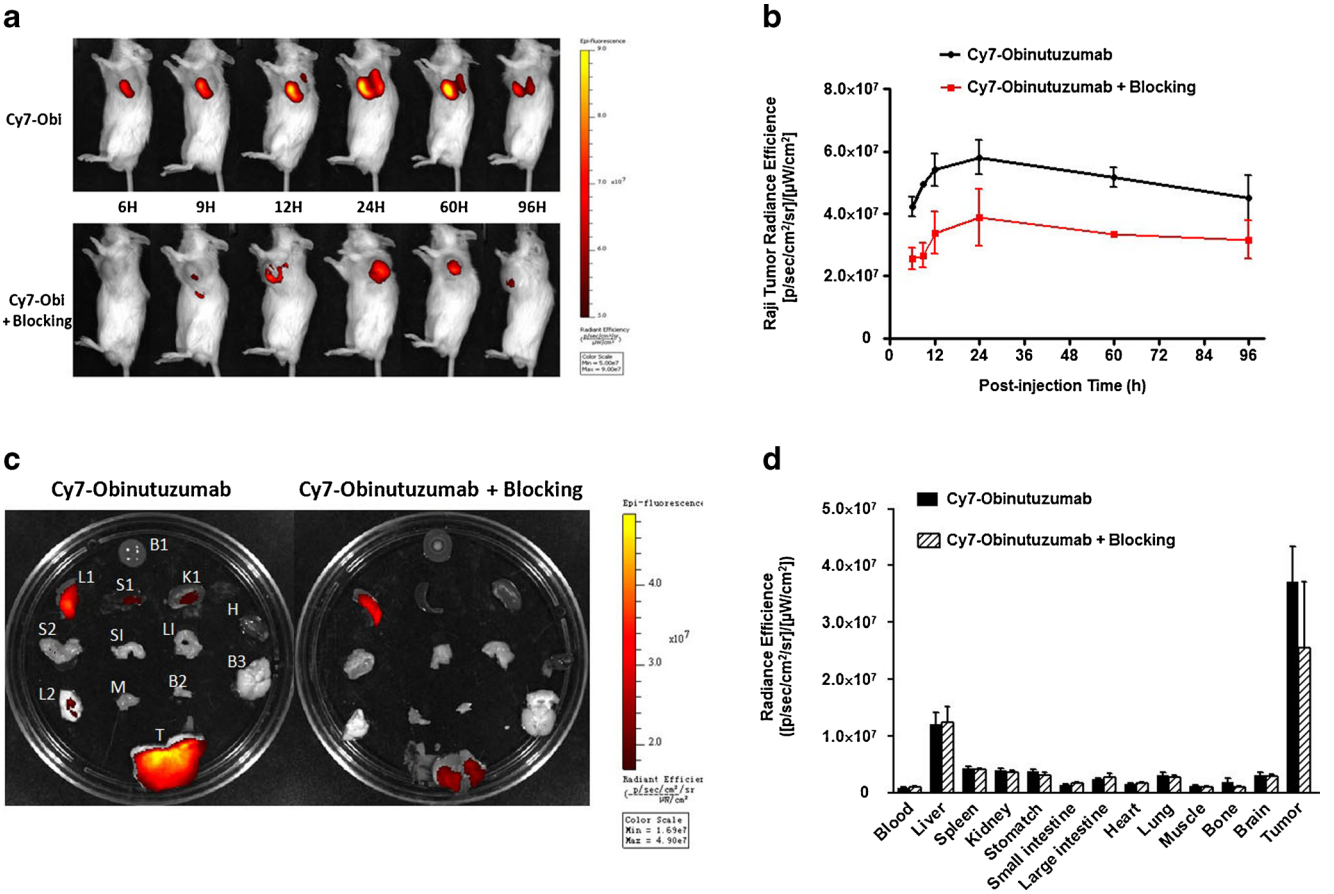

Fig. 4 **a** Representative *in vivo* fluorescence images of the mice bearing Raji tumor injected with Cy7-Obi (1 nmol) with and without pre-blocking of obinutuzumab (3.25 mg). **b** The time–activity curve of fluorescence intensity ([p/s/cm^2/sr]/[μW/cm^2]) at the Raji tumor with (*red square*) and without (*black circle*) pre-blocking of obinutuzumab. **c** *Ex vivo* NIRF imaging of the dissected Raji tumor and major organs. **d** Biodistribution data, with and without pre-blocking by obinutuzumab 96 h post-injection (three mice per group). *B1* blood, *L1* liver, *S1* spleen, *K1* kidney, *S2* stomach, *SI* small intestine, *LI* large intestine, *H* heart, *L2* lung, *M* muscle, *B2* bone, *B3*, brain, *T* Raji tumor.

analysis (see ESM). The UV–vis spectrum showed that the conjugate has the two characteristic peaks at 280 and 750 nm: the first peak is the characteristic peak which originated from obinutuzumab, and the second peak is the characteristic peak which originated from Cy7-NHS. This feature provided the basis to calculate the *F*/*P* ratio of the conjugate. The number of Cy7 moiety from the conjugate was clearly observed from MALDI-TOF mass spectrum, the difference of the mass between the conjugate, and obinutuzumab reflecting the number of Cy7. No other heavier or lighter molecule peaks were observed, showing relative rather simple composition of the conjugate. SDS-PAGE analysis showed that the conjugate had the molecular weight close to that of obinutuzumab and showed the fluorescent peak similar to that of Cy7-NHS (see ESM Fig. 3). All these pieces evidence show that the conjugate has the combined properties of obinutuzumab and Cy7-NHS within a single molecule.

The affinity of the conjugate Cy7-Obi to CD20 closely resembles that of obinutuzumab, which has been demonstrated in the experiments (Fig. 2). The specificity of the conjugate is examined by *in vitro* microscopy and histology. Fluorescence microscopy image showed significant fluorescent signal when the CD20-expressing cells were incubated with the conjugate, while the signal was blocked by pretreatment with obinutuzumab (Fig. 3). Immunofluorescence imaging showed that the conjugate accumulated within the cell membrane of the Raji tumor cells, while the CD20 antigen was specifically blocked by murine monoclonal antibody (Fig. 5). All these experiments show that the conjugate Cy7-Obi has the same affinity and specific binding as obinutuzumab.

The conjugate Cy7-Obi was used in the NIRF imaging of living mice bearing Raji tumors. Cy7-Obi within the tumor was clearly observable 6 h p. i. and had a maximal absorption at 24 h p. i. (Fig. 4a, b). The specific signal within the tumor was blocked by pretreatment with obinutuzumab. The *in vivo* results were confirmed through *ex vivo* experiments of dissected organs (Fig. 4c, d). This study demonstrated that Cy7-Obi showed displaceable specific signal within tumor, showing promise as a near-infrared imaging agent.

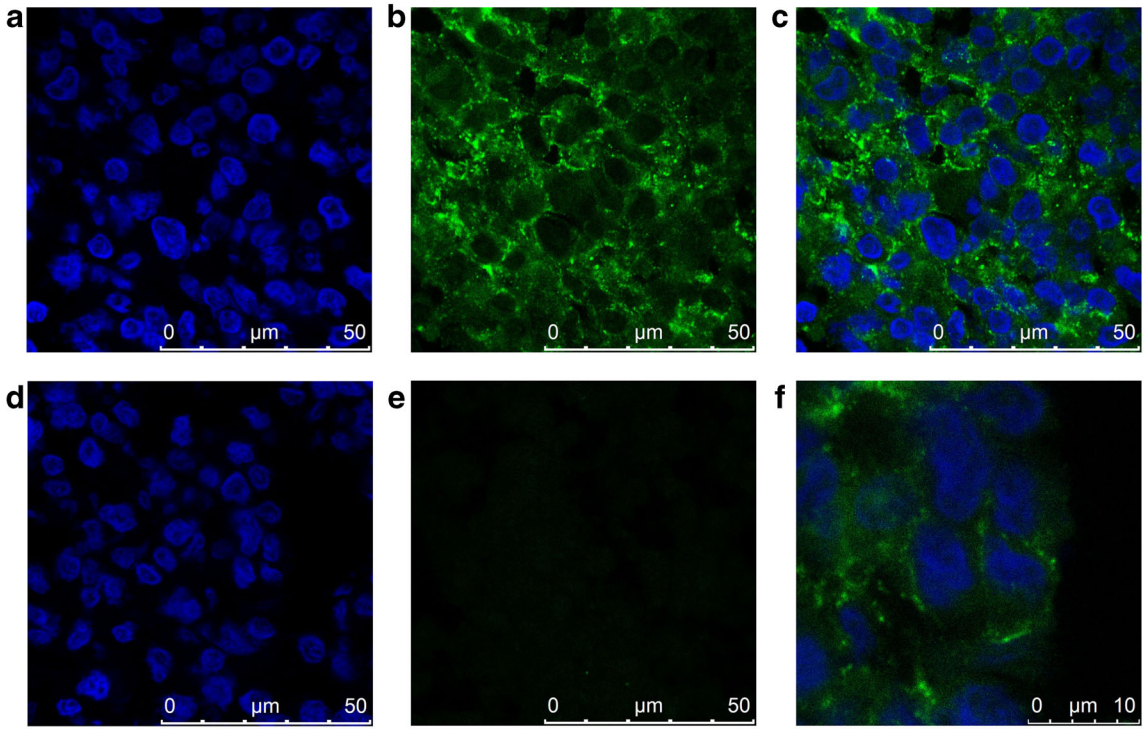

Fig. 5 Immunofluorescence imaging of the Raji tumor tissue, where the tissue slices for **a**–**c** and **f** were from Cy7-Obi-treated mice and for **d**–**e** from murine monoclonal antibody IgG-treated mice. **a**, **d** Cell nuclei stained with DAPI in *blue*. **b, e** Cell membrane stained with FITC-conjugated goat anti-human IgG in *green*. **c** Merged images of **a** and **b. f** Magnified view of **c**. All the images were acquired under the same conditions.

In order to evaluate the Cy7-Obi as a novel NIRF imaging agent in human NHL, the distribution in various organs especially in tumors is needed in animal models prior to human patient studies [39]. The uptake of Cy7-Obi 96 h post-injection was predominantly in the tumor, followed by that of the liver. Other organs have much less activity.

It needs to be emphasized that the blocking study aims not only to determine the binding specificity of the conjugate but also to search for ways to solve the problem of antibody accumulation in antigen sinks such as the spleen (The phenomenon has been noticed in our previous study [35]). Antigen sinks can "sop up" antibody, resulting in lower serum antibody levels and more rapid clearance. So, it is necessary to do pre-blocking clinically to avoid accumulation of antibody in the spleen. Successfully pre-blocking may allow for more mAb-based conjugate to circulate, thus increasing the availability to target NHL cells. In this study, the difference of fluorescence signal in the spleen between the mice of the blocked and unblocked group was not significantly large (Fig. 4d). The main reason lays in the mouse model we used [40]. SCID mice had mean absolute deficiency in immunosystem and lymphocyte malfunction, thus causing the loss of CD20 antigens. So, subsequent studies of Cy7-Obi may be performed in mice with normal immunosystem. In the same argument, to minimize antibody in the sinks, pre-blocking with cold rituximab was practiced clinically during the therapy with ^{90}Y-labeled Zevalin (a CD20 targeting antibody) [16].

Besides high uptake in tumor, the liver region also exhibited significant fluorescence activity in the mice injected with or without obinutuzumab. The uptake may come from the interaction of the Fc receptors present on the antibody with hepatocytes [21].

The conjugate showed excellent stability in serum study, presumably the same stability may maintain *in vivo*, allowing long and real-time imaging.

The new tracer, Cy7-Obi, has the potential for early detection of metastatic lymph nodes of NHL, thus contributing to the early diagnosis and staging. NHL is a heterogeneous group of malignancy of the lymphoid system. Its early and most common clinical manifestation is the painless and progressive enlargement of superficial lymph nodes. The diagnosis of NHL depends on pathological results. The accurate pathological diagnosis comes from complete lymph node biopsies. When some painless enlargements of lymph nodes occur and clinical symptoms are highly suspicious of NHL, lymph node biopsies will be performed. However, these abnormal lymph nodes can be caused by various kinds of pathogenic factors, such as inflammation, metastasis of tumor cells, and so on [41]. It is worthwhile to explore how to successfully detect the metastatic lymph nodes by rapid, exact, and noninvasive procedures, thus avoiding damage caused by blind biopsy.

Conclusions

In conclusion, we have developed a facile synthesis of a new conjugate, Cy7-Obi. The conjugate has been fully characterized and evaluated *in vitro*, *in vivo*, and *ex vivo*. The conjugate maintained the specificity of obinutuzumab, allowing NIRF imaging of CD20 in cell lines and in animal model of NHL overexpressing CD20. High uptake of Cy7-Obi was observed in tumor. Despite limitation of tissue penetration in some deep organs, strong fluorescence signal of Cy7-Obi was still detectable in subcutaneous transplanted tumors as well as the superficial metastatic lymph nodes. It has the potential to serve as an effective tool for noninvasive imaging to help to make early diagnosis and staging of NHL and even for *in vivo* monitoring of NHL growth and metastasis.

Acknowledgments. We thank the staff in Central Laboratory and Laboratory Animal Unit at Peking University Cancer Hospital & Institute and Dr. Xiaolong Liang in the Department of Biomedical Engineering at the College of Engineering in Peking University for instrumentation support and analysis. This work was supported by the National Natural Science Foundation of China (No. 81071198, No. 81172083, No. 81371592), Beijing Natural Science Foundation (No. 7132040), and Peking University Cancer Hospital& Institute Research Foundation (2013 ZiZhu 12).

Conflict of Interest. The authors declare that they have no conflicts of interest.

References

1. Siegel R, Naishadham D, Jemal A (2013) Cancer statistics, 2013. CA: A Cancer Journal for Clinicians 63:11–30
2. Alexander DD, Mink PJ, Adami HO et al (2007) The non-Hodgkin lymphomas: a review of the epidemiologic literature. Int J Cancer 120:1–39
3. Mohrbacher A (2005) B cell non-Hodgkin's lymphoma: rituximab safety experience. Arthritis Res Ther 7:S19–S25
4. Tedder TF, Engel P (1994) CD20: a regulator of cell-cycle progression of B lymphocytes. Immunol Today 15:450–454
5. Polyak MJ, Li H, Shariat N, Deans JP (2008) CD20 homo-oligomers physically associate with the B cell antigen receptor. Dissociation upon receptor engagement and recruitment of phosphoproteins and calmodulin-binding proteins. J Biol Chem 283:18545–18552
6. Kawabata KC, Ehata S, Komuro A et al (2013) TGF-β-induced apoptosis of B-cell lymphoma Ramos cells through reduction of MS4A1/CD20. Oncogene 32:2096–2106
7. Einfeld DA, Brown JP, Valentine MA et al (1988) Molecular cloning of the human B cell CD20 receptor predicts a hydrophobic protein with multiple transmembrane domains. EMBO J 7:711–717
8. Press OW, Appelbaum F, Ledbetter JA et al (1987) Monoclonal antibody 1F5 (anti-CD20) serotherapy of human B cell lymphomas. Blood 69:584–591
9. Anderson KC, Bates MP, Slaughenhoupt BL et al (1984) Expression of human B cell-associated antigens on leukemias and lymphomas: a model of human B cell differentiation. Blood 63:1424–1433
10. Perz J, Topaly J, Fruehauf S et al (2002) Level of CD 20-expression and efficacy of rituximab treatment in patients with resistant or relapsing B-cell prolymphocytic leukemia and B-cell chronic lymphocytic leukemia. Leuk Lymphoma 43:149–151
11. Cheson BD, Leonard JP (2008) Monoclonal antibody therapy for B-cell non-Hodgkin's lymphoma. N Engl J Med 359:613–626
12. Robak T (2009) GA-101, a third-generation, humanized and glyco-engineered anti-CD20 mAb for the treatment of B-cell lymphoid malignancies. Curr Opin Investig Drugs 10:588–596
13. Janice MR (2011) Antibody-based therapeutics to watch in 2011. MAbs 3:76–99
14. Stopar TG, Mlinaric-Rascan I, Fettich J et al (2006) ^{99m}Tc-rituximab radiolabelled by photo-activation: a new non-Hodgkin's lymphoma imaging agent. Eur J Nucl Med Mol Imaging 33:53–59
15. Gmeiner ST, Fettich J, Zver S et al (2008) ^{99m}Tc-labelled rituximab, a new non-Hodgkin's lymphoma imaging agent: first clinical experience. Nucl Med Commun 29:1059–1065
16. Natarajan A, Gowrishankar G, Nielsen CH et al (2012) Positron emission tomography of ^{64}Cu-DOTA-Rituximab in a transgenic mouse model expressing human CD20 for clinical translation to image NHL. Mol Imaging Biol 14:608–616
17. Olafsen T, Betting D, Kenanova VE et al (2009) Recombinant anti-CD20 antibody fragments for small-animal PET imaging of B-cell lymphomas. J Nucl Med 50:1500–1508
18. Olafsen T, Sirk SJ, Betting DJ et al (2010) ImmunoPET imaging of B-cell lymphoma using ^{124}I-anti-CD20 scFv dimers (diabodies). Protein Eng Des Sel 23:243–249
19. Biffi S, Garrovo C, Macor P et al (2008) *In vivo* biodistribution and lifetime analysis of cy5.5-conjugated rituximab in mice bearing lymphoid tumor xenograft using time-domain near-infrared optical imaging. Mol Imaging 7:272–282
20. Wu Y, Cai W, Chen X (2006) Near-infrared fluorescence imaging of tumor integrin $\alpha_v\beta_3$ expression with Cy7-labeled RGD. Mol Imaging Biol 8:226–236
21. Sampath L, Kwon S, Ke S et al (2007) Dual-labeled trastuzumab-based imaging agent for the detection of human epidermal growth factor receptor 2 overexpression in breast cancer. J Nucl Med 48:1501–1510
22. Kim TI, Park J, Park S et al (2011) Visualization of tyrosinase activity in melanoma cells by a BODIPY-based fluorescent probe. Chem Commun (Camb) 47:12640–12642
23. Vinegoni C, Botnaru I, Aikawa E et al (2011) Indocyanine green enables near-infrared fluorescence imaging of lipid-rich, inflamed atherosclerotic plaques. Sci Transl Med 3(84):84ra45
24. Jensen SA, Day ES, Ko CH et al (2013) Spherical nucleic acid nanoparticle conjugates as an RNAi-based therapy for glioblastoma. Sci Transl Med 5(209):209ra152
25. van der Poel HG, Buckle T, Brouwer OR et al (2011) Intraoperative laparoscopic fluorescence guidance to the sentinel lymph node in prostate cancer patients: clinical proof of concept of an integrated functional imaging approach using a multimodal tracer. Eur Urol 60:826–833
26. Greg TH (2008) Bioconjugate techniques. In: Greg TH (ed) Fluorescent probes. Academic, San Diego, pp 396–405
27. Morrison LE (2008) Basic principles of fluorescence and energy transfer. Methods Mol Biol 429:3–19
28. Marras SA, Kramer FR, Tyagi S (2002) Efficiencies of fluorescence resonance energy transfer and contact-mediated quenching in oligonucleotide probes. Nucleic Acids Res 30:e122
29. Miller JN (2005) Fluorescence energy transfer methods in bioanalysis. Analyst 130:265–270
30. Brun MP, Gauzy-Lazo L (2013) Protocols for lysine conjugation. Methods Mol Biol 1045:173–187
31. Anders JC, Parten BF, Petrie GE et al (2003) Using amino acid analysis to determine absorptivity constants: a validation case study using bovine serum albumin. Biopharm International 16:30–37
32. Van Meerten T, van Rijn RS, Hol S et al (2006) Complement-Induced cell death by rituximab depends on CD20 expression level and acts complementary to antibody-dependent cellular cytotoxicity. Clin Cancer Res 12:4027–4035
33. Wu L, Wang C, Zhang D et al (2010) Characterization of a humanized anti-CD20 antibody with potent antitumor activity against B-cell lymphoma. Cancer Lett 292:208–214
34. Aoki V, Sousa JX Jr, Fukumori LM et al (2010) Direct and indirect immunofluorescence. An Bras Dermatol 85:490–500
35. Lin X, Zhu H, Hong Y et al (2013) Synthesis and evaluation of Cy7-Rituximab targeting CD20 antigen for *in vivo* animal fluorescence imaging. Chem J Chinese U 34:2139–2145
36. Natarajan A, Habte F, Liu H et al (2013) Evaluation of ^{89}Zr-rituximab tracer by Cerenkov luminescence imaging and correlation with PET in a humanized transgenic mouse model to image NHL. Mol Imaging Biol 15:468–475
37. Tang B, Cui L, Xu K et al (2008) A sensitive and selective near-infrared fluorescent probe for mercuric ions and its biological imaging applications. Chembiochem 9:1159–1164

38. Zhang Y, Hong H, Engle JW et al (2012) Positron emission tomography and near-infrared fluorescence imaging of vascular endothelial growth factor with dual-labeled bevacizumab. Am J Nucl Med Mol Imaging 2:1–13
39. Dixit R, Boelsterli UA (2007) Healthy animals and animal models of human disease(s) in safety assessment of human pharmaceuticals, including therapeutic antibodies. Drug Discov Today 12:336–342
40. Mashimo T, Takizawa A, Kobayashi J et al (2012) Generation and characterization of severe combined immunodeficiency rats. Cell Rep 2:685–694
41. Ghirardelli ML, Jemos V, Gobbi PG (1999) Diagnostic approach to lymph node enlargement. Haematologica 84:242–247